Theoretical and Applied Fracture Mechanics 53 (2010) 1–8

Contents lists available at ScienceDirect

Theoretical and Applied Fracture Mechanics

journal homepage: www.elsevier.com/locate/tafmec

Axial compression and energy absorption characteristics of high-strength thin-walled cylinders under impact load

Y.S. Tai [a,*], M.Y. Huang [b], H.T. Hu [b]

[a] Department of Civil Engineering, ROC Military Academy, Taiwan, ROC
[b] Department of Civil Engineering, National Cheng Kung University, Taiwan, ROC

ARTICLE INFO

Article history:
Available online 16 December 2009

Keywords:
High-strength steel
Impact
Axial compression
Thin-walled cylinders

ABSTRACT

Non-linear finite element software LS-DYNA is used to analyze the axial compression behavior and energy absorption of a high-strength thin-walled member under an impact load. To elucidate the effect of dynamic impact on the strain rate, the Cowper–Symonds equation is applied to analyze the plastic state of stress and the onset of dynamic yielding under different strain rates, such that the modeled deformation behavior of the member is consistent with the actual situation. Results for the thin-walled members made of mild steel and dual phase steel are compared. Assuming two different materials with equal sectional areas, an analysis confirms that the energy absorption of high-strength steel thin-walled component is better than the mild steel thin-walled component. Hence, thin-walled tubes made of high-strength steel are investigated using a series of analysis. The relationships between displacement and load, average load and energy absorption properties are obtained.

1. Introduction

Industrial progress and energy shortage have called for the auto manufactures to produce lighter vehicles but not at the expense of safety under impact. This can be accomplished by using light materials with higher ultimate strength. Appropriate candidates are thin-walled members because they are superior in absorbing energy. This increases the impact durability. Many researchers have developed various models for analyzing the axial bucking property of thin-walled members based on the plastic hinge theory [1–5], experimentation or numerical simulation [6–17]. The work in [1] observed the accordion-like axisymmetric deformation pattern of a cylinder under plastic buckling during an experiment, and proposed the concept of the static plastic hinge. The destruction pattern of the cylinder under axial compression suggested a model, simple in calculation while the results for energy absorption are consistent with those found from experiments. The work in [6] performed a series of tests on an aluminum-alloy thin-walled cylindrical tube with a D/t ratio of 4–60 and an L/D ratio of 0.2–8.8. Identified experimentally were different destruction patterns using different D/t and L/D ratios. Presented in [7] adopt the non-linear finite element code of ABAQUS to analyze an aluminum-alloy rectangular thin-walled structure, determining the effect of the impact speed and the impact masses on the axial buckling behavior of thin-walled tubes. In the simulation, the property of aluminum was found to be insensitive to the strain rate which was consistent with the experimental results. It was also found that the discrepancy between the dynamic buckling behaviors of cylindrical and rectangular tubes was mainly associated with the transmission of the stress wave in the structure of different geometric shapes. The work in [8] divided the plastic buckling of a cylindrical shell under axial loading into dynamic progressive buckling and dynamic plastic buckling. When a structure sustains a slower impact, members from one end to the other gradually develop overlapping shrinkage, which process is called dynamic progressive buckling. Dynamic plastic buckling is an overall buckling behavior that is caused by the repeated reflection of the stress wave when the structure is under an impact of high-velocity. Conducted in [9] were impact tests on a rectangular AA6060 aluminum-alloy structure. Taking into account the fact that the members were initially imperfect, they investigated the effect of impact mass and impact speed on the energy absorbing behavior of the tubes. They also utilized LS-DYNA to analyze the dynamic response of the aluminum tube to impacts of various speeds and masses. Experimental results were consistent with the destruction pattern and the energy absorbing properties. LS-DYNA were employed [10] to scrutinize hat-shaped sections of various materials, analyzing in detail the effect of the height and initial imperfection of the hat-shaped member on its axial compression behavior. The compression behaviors of an aluminum-alloy cylindrical tube have been tested [11] which also developed a numerical model that is consistent with experiments. Moreover, the adopted analytical model was used to study the effect of initial imperfection and

* Corresponding author. Tel.: +886 7 7456290; fax: +886 7 7104697.
E-mail address: ystai@cc.cma.edu.tw (Y.S. Tai).

0167-8442/$ - see front matter © 2009 Elsevier Ltd. All rights reserved.
doi:10.1016/j.tafmec.2009.12.001

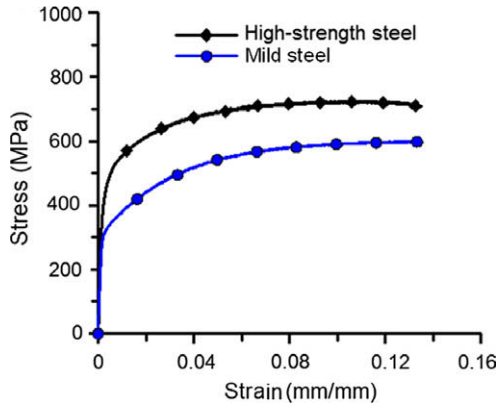

Fig. 1. Stress–strain characteristic of the steel.

material strain rate on the axial compression behavior of a thin-walled cylindrical tube. Recent works [12] performed dynamic tensile tests to plot the stress–strain curve of material at various strain rates. The Cowper–Symonds equation were modified form the dynamic parameters to establish a numerical model of thin-walled members made of TRIP and dual phase steel. The findings revealed that the modified dynamic parameters can effectively simulate the deformation behavior of a thin-walled member under impact loading. Others have also examined the influence of the geometric shape of a thin-walled member on its buckling behavior and absorption characteristics [13,14].

Dual phase steel is a high-strength steel [18]. Its higher strength and durability are enabling it to gradually replace conventional steel materials and to play an important role in transportation, the aerospace industry and bridge structures, as well as in military facilities, as it increases the crashworthiness and energy absorbing capacity of structures that are constructed from it. In what follows, the non-linear finite element software LS-DYNA is used to investigate the dynamic compression behavior and energy absorbing property of high-strength thin-walled tubes under various impact masses and impact velocities, taking into account the strain rate and geometric thickness of the material.

2. Mechanical characteristics of material

The mechanical behavior of high-strength thin-walled tubes under impact loading was simulated by using the ASTM E8-04, MTS 819 50 kN multi-purpose oil hydraulic machine for quasi-static tensile tests in close-loop control mode. During the test, a strain gage is attached to the sample to measure strain signals. To identify differences between high-strength steel and conventional steel, the uniaxial tensile tests were conducted. Fig. 1 plots the typical stress-strain curves of both materials. The yield stresses determined by the 0.2% offset method are 446 and 325 MPa, respectively. Young's modulus was determined from the slope of the line determined by linear regression between $0.1\,\sigma_y$ and $0.9\,\sigma_y$, and was 207.2 GPa. The curves for different strain rates can be obtained from the Cowper–Symond equation

When a structure is under a dynamic load, it deforms rapidly, its stress–strain relationship determines the value of the strain, and assumes the change to be inversely proportional. Many investigations have considered various constitutive laws concerning the strain rate's influence on material properties [8,12,19,20]. When the stress–strain relationship using regression formula is obtained from the dynamic load of the material, the constitutive law of the material is found. Material parameters for the constitutive law are obtained every time for a specific situation while a regression analysis is performed on the test results. A simple equation [21] is used to obtain the dynamic yield stress from the static strength:

$$\dot{\varepsilon} = D\left(\frac{\sigma_{dy}}{\sigma_y} - 1\right)^n \qquad \sigma_{dy} > \sigma_y \qquad (1)$$
$$\sigma_{dy} = \sigma_y\left[1 + |\dot{\varepsilon}/D|^{1/n}\right]$$

where $\dot{\varepsilon}$ denotes the truth strain rate; σ_{dy} denotes the rate related to the dynamic yield stress; σ_y represents the static yield stress; D and n represent the material parameters. It was shown for steel [22] with $D = 40\,s^{-1}$ and $n = 5$ that the predicted results and experimental data agree.

Table 1
The specimen geometry and test detail.

Model	Parameters Wall thickness 0.6, 0.8, 1.0 mm; Free length (L_0) 90, 120, 200 mm						
	Type	Length (mm)	Thickness (mm)	Diameter (mm)	Impact mass (kg)	Impact velocity (m/s)	Impact energy (kJ)
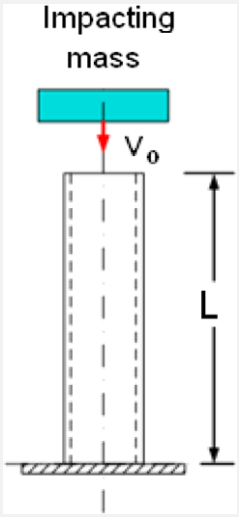	HS-01	120	0.6	31	10	10	0.5
	HS-02	120	0.6	31	20	10	1.0
	HS-03	120	0.6	31	30	10	1.5
	HS-04	120	0.6	31	40	10	2.0
	HS-05	120	0.6	31	50	10	2.5
	HS-06	90	0.8	31	30	10	1.5
	HS-07	90	0.8	31	30	15	3.4
	HS-08	90	0.8	31	30	20	6.0
	HS-10	90	0.8	31	200	5.48	3.0
	HS-11	90	0.8	31	100	7.75	3.0
	HS-12	90	0.8	31	25	15.49	3.0
	HS-13	90	0.8	31	10	24.49	3.0
	HS-14	90	0.6	31	30	10	1.5
	HS-15	90	1.0	31	30	10	1.5
	HS-16	90	0.6	31	30	15	3.4
	HS-17	90	1.0	31	30	15	3.4
	HS-18	90	0.6	31	30	20	6.0
	HS-19	90	1.0	31	30	20	6.0
	HS-20	200	1.0	31	30	15	3.4
	HS-21	200	0.67	46.5	30	15	3.4
	HS-22	200	0.5	62	30	15	3.4

Table 2
The material parameters.

			Density (kg/m^3)		E (GPa)			SIGY(MPa)
High-strength steel			7820		207.2			446
Mild steel			7820		207.2			325
High-strength steel								
Stress (MPa)	446.0	496.6	563.1	612.7	664.2	691.5	717.8	714.4
Strain (m/m)	0.0	0.00183	0.00805	0.01678	0.0321	0.0481	0.0819	0.1304
Mild steel								
Stress (MPa)	325.0	450.6	511.8	564.9	597.6	594.9	584.3	572.3
Strain (m/m)	0.0	0.0187	0.0343	0.0613	0.1229	0.1505	0.1640	0.1721

3. Analytical model

Under axial compression, a thin-walled tube absorbs the impact energy by plastic deformation. The destruction mode influences its energy absorbing efficiency. Therefore, understanding the characteristics of the process in which thin-walled tubes are compressed can help to elucidate effectively the dynamic response of thin-walled components under high-velocity impact. It was found [23] that under high-velocity dynamic loading, the deformation of the cylinder is significantly associated with the impact speed, inertia of the impact mass, geometric configuration and material property. While addressing the effect of the material properties for different impact speed, the corresponding mass and the geometric configuration of the structure is also considered to understand the energy absorbing property of a thin-walled tube.

Non-linear finite element code, LS-DYNA, was employed to analyze the destruction pattern and energy absorbing properties of thin-walled components with circular sections under axial impact loading. The diameter of the circular tubes was 31 mm. Circular tubes of various lengths and wall thicknesses were numbered, as presented in Table 1. Simulation using a whole model was used for analysis because of uncertainty in the destruction pattern. According to past investigation [24], to display fully the buckling pattern of the structure and to make the outcome of the simulation more consistent with actual overlapping compression, the mesh must be smaller than half of the stress wavelength or the length of the plastic hinge. The half-length of the stress wavelength is,

$$l = \pi \frac{\sqrt{Rt}}{\sqrt[4]{12(1-v^2)}} \tag{2}$$

where R and t represent the diameter and thickness of the cylinder tube, respectively, and v denotes the Poison ratio of the material. The length of the plastic hinge during buckling is computed using the formula of the [25],

$$h = 1.76\sqrt{\frac{Rt}{2}} \tag{3}$$

Since the minimum thickness of the thin-walled components in this investigation is 0.6 mm, Eqs. (2) and (3) yield an optimal mesh size of 2.0 mm. All the tubes are modeled using Belytschko–Tsay four-node shell elements with five integration points through the thickness and one integration point in the element plane. The meshed shell elements were located at the mid-surface of the tube's wall. The stiffness-type hourglass control model is adopted to eliminate the zero-energy modes.

The Type 24 Piecewise Linear Plasticity constitutive law of LS-DYNA is employed. The primary advantage of the material lies in the fact that it can simultaneously display completely the characteristics of the plastic phase and take into account the effect of the strain rate. Table 2 presents the parameters of the materials that are used in the constitutive law.

For simulation of the dynamic axial crushing, the bottom end of the tube is assumed to be built-in and is constrained in all degrees of freedom. The upper end was free and subject to compression by the rigid loading plate with certain downward initial velocity of V_0. The loading plate is modeled as a rigid wall with a mass of m_0. To prevent penetration and sliding between the rigid loading plate and the upper end of the tube during contact, the interface is using the CONTACT_CONSTRAINT_NODES_TO SURFACE command of LS-DYNA. The interface force between the rigid loading plate and the tube was used to obtain the force vs. displacement responses. The friction coefficient between the contact surfaces is set to 1.0. Furthermore, when the thin-walled tube experiences overlapping shrinkage, the contact property between the lobes is CONTACT-AUTOMATIC-SINGLE-SURFACE with a friction coefficient of 0.1, preventing the lobes from penetrating each other during the deformation process.

4. Results and discussion

The mechanical behavior of a high-strength is considered for thin-walled cylinder steel tube under axial impact. The energy absorbing efficiencies of this material and traditional steel are compared. Energy absorbing capacity can generally be measured as the mass-specific energy absorption in the effective destruction length of the structure. It is defined as follows;

$$E_s = \frac{E_{total}}{\Delta M} = \frac{E}{A\Delta L\rho} \tag{4}$$

where ΔM is the mass in the crushing length of the cylindrical tube, E_{total} is the total energy absorbed in the crushing process, ΔL represents the effective crushing length, ρ is density and A is the cross-sectional area of the cylinder tube. Fig. 2 displays the mass-specific energy absorption of mild steel and high-strength steel tubes of a

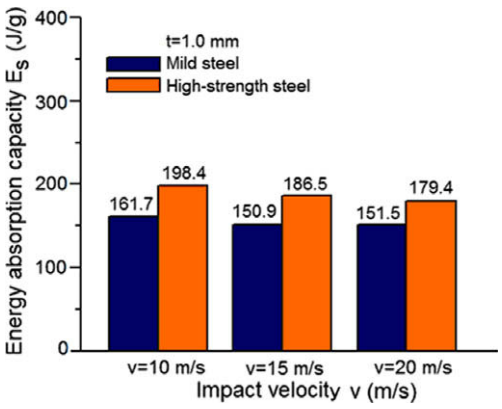

Fig. 2. Energy absorption capacity of the mild steel and high-strength steel tubes under various impact velocities.

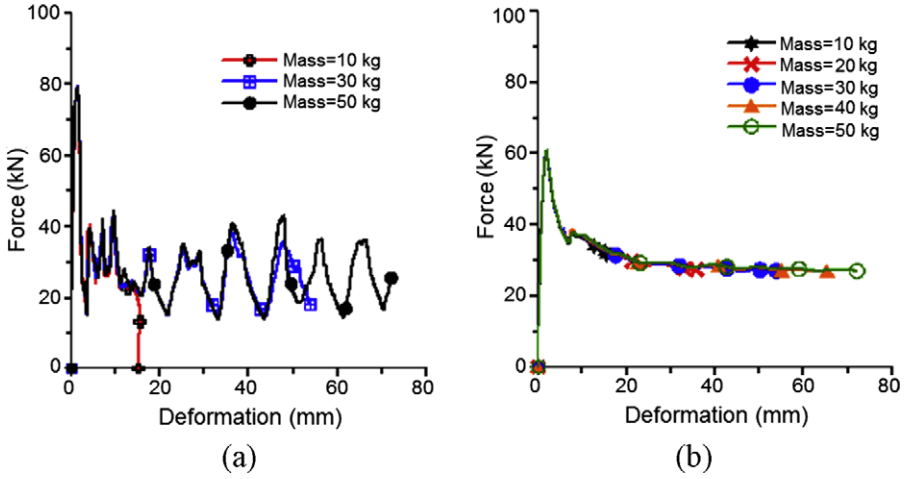

Fig. 3. Axial crushing behavior of the high-strength steel tubes with different impact mass (a) force vs. deformation curve and (b) mean force vs. deformation curve.

thickness of 1.0 mm under impact at three speeds, and indicates that the mass-specific energy absorption of high-strength steel tube is 22.7%, 23.6% and 18.4% higher than that of mild steel, based on impact speed. The strain hardening effect of the material under high-speed impact increases the impact force and reduces deformation. Accordingly, for a particular crushing length, a high-strength steel tube has a higher energy absorbing capacity than conventional steel materials.The effect of the impact mass on the dynamic mechanical behavior of thin-walled components was analyzed for HS-01–HS-05 thin-wall tubes under the same impact speed (10 m/s) as the impact mass is varied between 10 and 50 kg. It also showed the relationship between the contact force (P) of the impact mass on the impact end of the thin-walled tube, the mean force (P_m) and the axial displacement, to elucidate the energy absorbing property of the structure. Here, the mean force (P_m) is given by,

$$P_m = \frac{E}{\delta} = \frac{\int P d\delta}{\delta} \tag{5}$$

$$E = \frac{1}{2} m v^2 \tag{6}$$

To clarify the results of the comparative, Fig. 3 plots the relationship between the contact force and the displacement under three impact masses (10, 30, 50 kg), and the relationship between the mean force and the displacement. Fig. 3 reveals that the peak loading is almost independent of the impact mass. The increase in displacement is also approximately independent of the impact mass. The only difference is observed in the second half of the curve. As the impact mass rises, it will causes a greater crushing deformation of the thin-walled tube and elongates it, as presented in Table 3. The kinetic energy formula explains this result. Restated, for a constant speed, if the mass increases, the kinetic energy increases, causing the thin-walled component to produce more folds and to deform more severely.

The work [26] is made use for the rectangular thin-walled components under impact loading, the deformation of a thin-walled component caused by the impact of a mass is similar to that caused by a nonlinear spring. The stiffness of the member and the impact mass are independent of each other. The dynamic loading caused by the impact mass and the deformation of the member are not directly to each other. Hence, for HS-01–HS-05 thin-walled compo-

Table 3
Summary of impact test results.

NO	Impact mass (kg)	Impact velocity (m/s)	Impact energy (kN)	Peak load (kN)	Displacement (mm)	Mean force (kN)	Energy absorption (kJ)	Mass-specific absorption (J/g)
HS-1	10	10	0.5	79.2	15.58	60.7	4.94	1387.8
HS-2	20	10	1.0	79.6	36.2	61.1	9.87	1193.4
HS-3	30	10	1.5	79.8	53.8	61.0	1.46	118.8
HS-4	40	10	2.0	79.6	65.2	61.0	1.76	118.1
HS-5	50	10	2.5	79.3	72.0	61.1	1.94	117.9
HS-6	30	10	1.5	116.3	31.3	92.0	1.48	155.2
HS-7	30	15	3.4	120.9	70.4	96.1	3.32	154.8
HS-8	30	20	6.0	123.7	82.3	98.6	5.64	225
HS-10	200	5.48	3.0	114.0	66.2	87.9	2.93	145.1
HS-11	100	7.75	3.0	116.0	65.8	90.2	2.94	146.6
HS-12	25	15.49	3.0	120.3	64.1	96.4	2.95	151.1
HS-13	10	24.49	3.0	126.1	60.3	101.4	2.95	160.6
HS-14	30	10	1.5	81.8	54.4	62.3	1.48	119.1
HS-15	30	10	1.5	147.0	19.6	120.0	1.48	198.3
HS-16	30	15	3.4	84.5	80.5	65.3	3.23	175.6
HS-17	30	15	3.4	151.6	49.7	124.9	3.24	176.5
HS-18	30	20	6.0	88.6	88.5	67.9	5.88	290.8
HS-19	30	20	6.0	155.6	78.4	129.1	5.84	195.6
HS-20	30	15	3.4	144.7	48.5	117.4	3.32	179.8
HS-21	30	15	3.4	128.3	83.6	89.6	3.32	104.3
HS-22	30	15	3.4	120.9	129.2	70.9	3.30	67.1

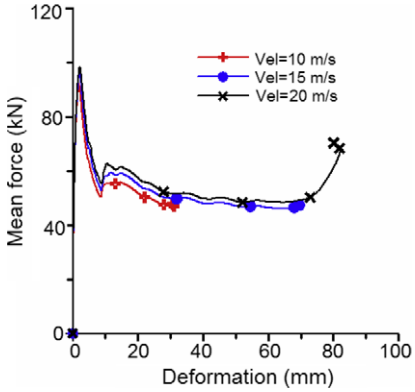

Fig. 4. Axial crushing behavior of the high-strength steel tubes with different impact velocities.

nents of fixed section area, the mean force-displacement curves do not vary significantly with impact mass, as presented in Fig. 3.

The initial impact speed is another important factor that influences the kinetic energy and the strain rate. The inertia of the members increases with the impact speed. First, for the HS-06–HS-08 thin-walled cylinder tubes, presented in Table 1, three impact speeds (10, 15, 20 m/s) are considered with a fixed impact mass of 30 kg. Fig. 4 plots the relationship between the average force and the displacement under three impact speeds. Figs. 5 and 6 plot the force and displacement curves, respectively, obtained at impact speeds, 15 and 20 m/s, and the corresponding deformations. Fig. 4 indicates that the displacement elongation of the thin-walled component and the numbers of folds are approximately independent of impact speed. Meanwhile, the peak loading increases slowly with the velocity, as presented in Table 3. This phenomenon becomes more significant as the speed increases be-

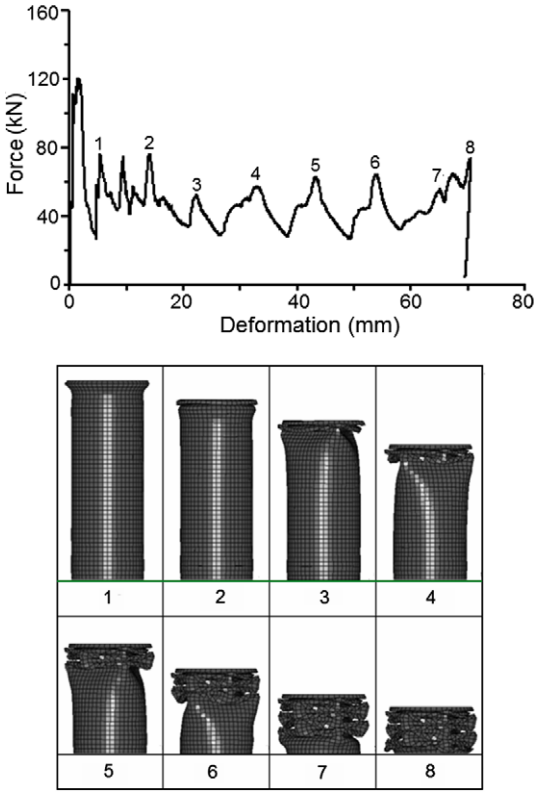

Fig. 5. Load-deformation history and collapse profiles of the HS-08.

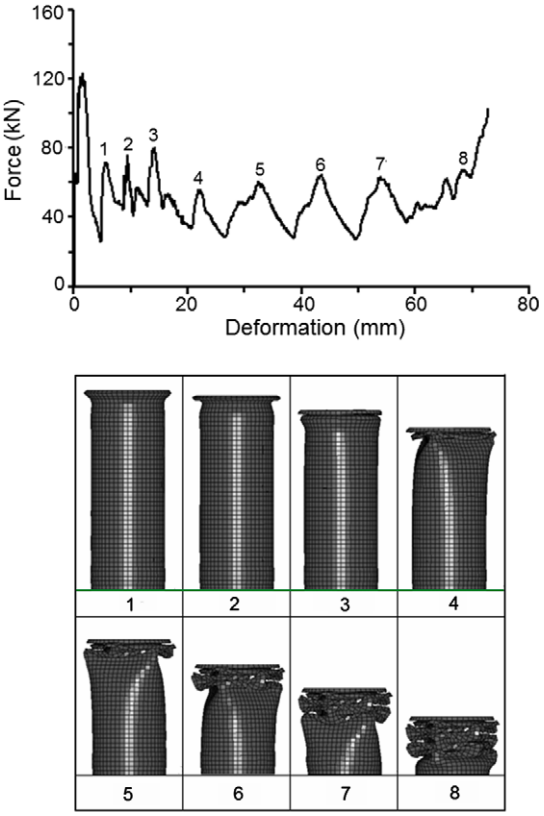

Fig. 6. Load-deformation history and collapse profiles of the HS-07.

cause changing the impact speed changes only the magnitude of the kinetic energy, but not the displacement elongation. The crushing process of the thin-walled component reveals that at initial speeds 10 and 15 m/s, the deformation of the thin-walled cylinder tube stops before it reaches the length of the axis, and a slight bounce-back of the mass is evident. When the initial speed is increased to 20 m/s, the thin-walled cylinder is slowly pressed down because changing the impact speed changes the kinetic energy, and the inertia and axial displacement increase with the speed.

An external impact causes the thin-walled cylindrical component to absorb the axial crushing energy. Since different impact speeds may be associated with the same impact kinetic energies,

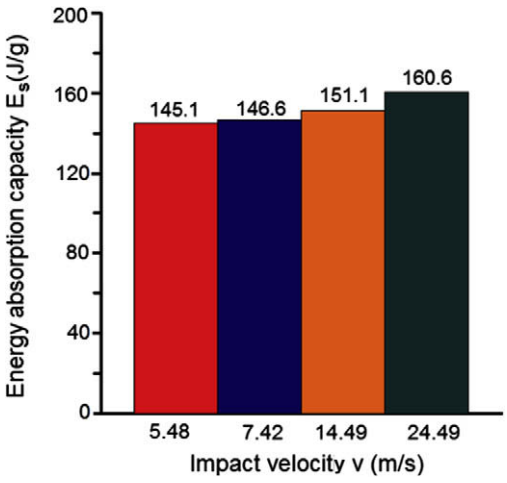

Fig. 7. Comparison of energy absorption capacity of the high-strength steel tubes under various velocities.

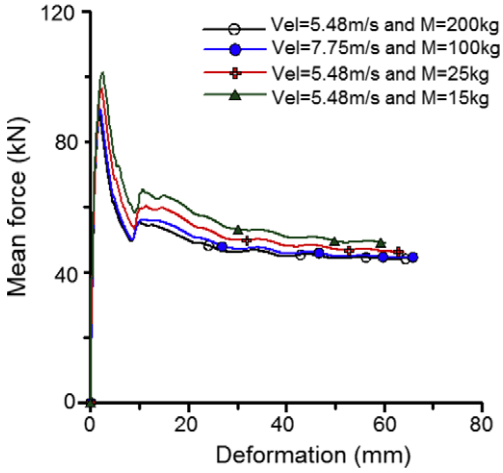

Fig. 8. The mean crushing force vs. deformation responses of the HS-10–HS-13.

the sensitivity of impact speed must be examined further. The so-called question of impact speed sensitivity refers to how the destruction pattern and axial compression displacement of the cylindrical tube change with the impact speed when the impact kinetic energy remains constant.

To understand further the effect of impact speed on the thin-walled component, HS-10–HS-13 thin-wall tubes are used and the specific energy absorption is obtained for various impact speeds, as presented in Fig. 7. When the impact energy is constant and the impact speed is increased, the specific energy absorption increases and the difference between the specific energy absorptions slowly increases also, indicating that indeed influence the energy absorption efficiency of thin-walled components, and warrants further study. Fig. 8 presents the relationship between the mean force and the displacement curve. When the impact energy is 3,000 J, the impact speed slowly increases and the peak value of the mean force also increases according to the figure. The only difference is that the crushing of the cylindrical tube stops at different positions relative to the bottom of the tube. This conclusion is supported by Figs. 9–12. If the component absorbs all of the impact energy, then the ultimate deformation of the component slowly declines as the impact speed increases.

Based on the mean force theory formulae, the two main factors influencing the mean force are thickness and diameter of the thin-walled tube. Restated, the section area in which the thin-walled tube receives the impact not only influences the ability of the component to resist deformation but also is associated with the energy absorbing efficiency. For a particular diameter, the section area

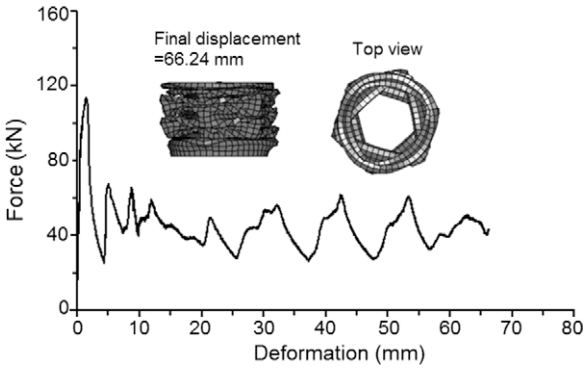

Fig. 9. The crushing responses of the HS-10.

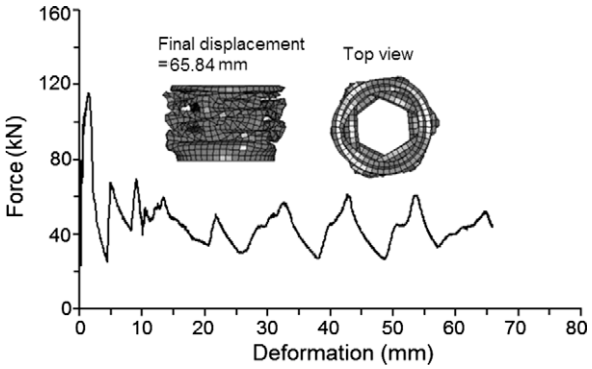

Fig. 10. The crushing responses of the HS-11

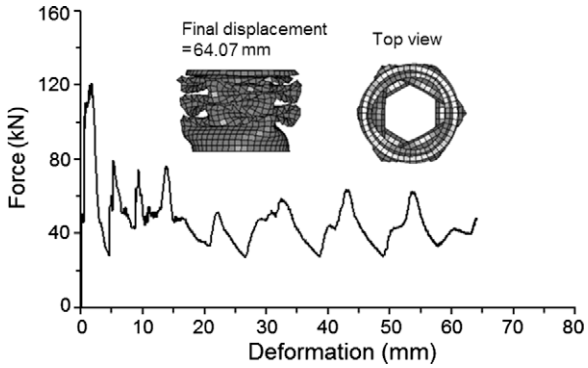

Fig. 11. The crushing responses of the HS-12.

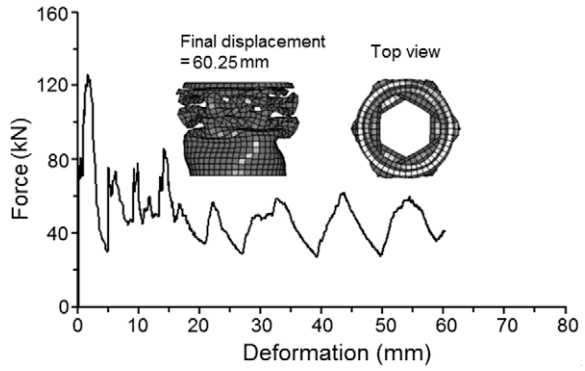

Fig. 12. The crushing responses of the HS-13.

varies with the thickness. Accordingly, to determine the effect of the thickness on the thin-walled component, HS-06, HS-14 and HS-15 are considered. Fig. 13 plots the energy-displacement curve obtained by the analysis. It indicates that for a particular speed and displacement, increasing the thickness of the wall increases the energy absorbing performance of the component. This finding is consistent with the conclusion of numerous studies, which have found that for a given wall thickness, the energy absorbing capacity of the component is proportional to the diameter of the cylindrical tube. The force vs. deformation curves of HS-06–HS-08 and HS-16–HS-19, plotted in Figs. 14–16, reveal this phenomenon.

With respect to the effect of axial length on the energy absorbing capacity, previous studies of cylindrical tubes have concluded that if not elongated to an extent that would cause the tube to buckle, and if not diminished in length beyond a certain extent,

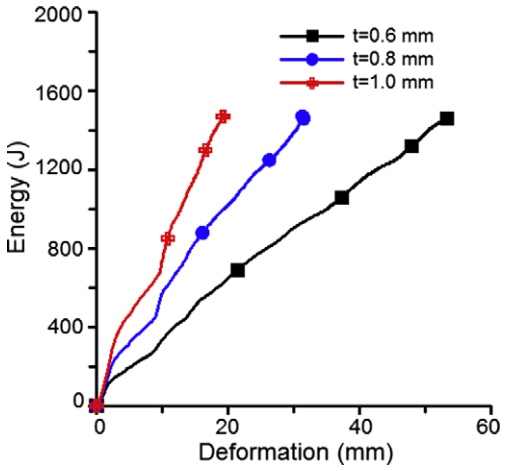

Fig. 13. Energy absorption vs, axial crushing displacement.

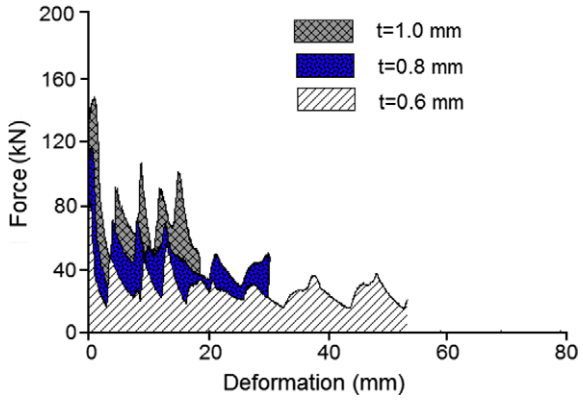

Fig. 14. The crushing force vs. deformation responses of the HS-06, HS-14 and HS-15.

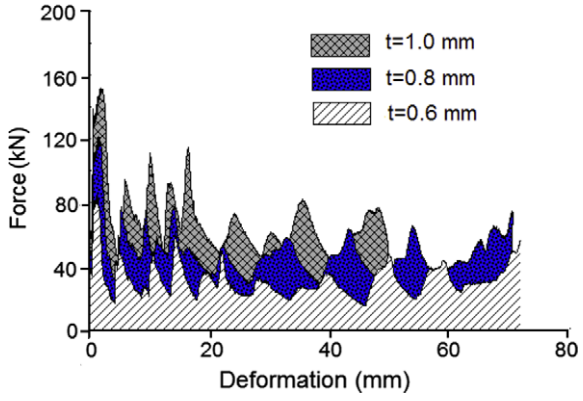

Fig. 15. The crushing force vs. deformation responses of the HS-07, HS-16 and HS-17.

the axial length does not influence the energy absorbing performance, because when both the kinetic energy and the geometry of the component are constant, they cause constant deformation. Hence, the effect of the axial length is negligible.

Further considerations of the energy absorbing efficiency of the thin-walled component are the solidity ratio of the structure. This reveals how the size of the member influences energy absorbing efficiency. The solidity ratio is defined as,

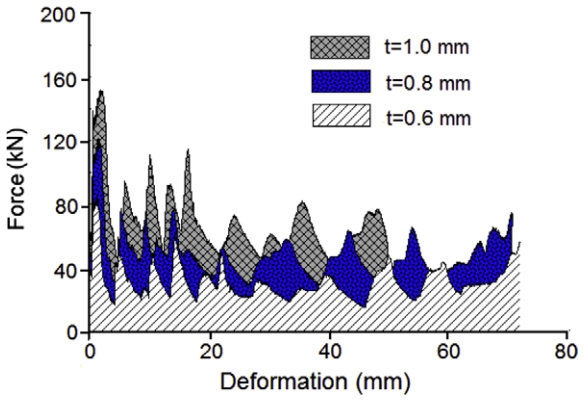

Fig. 16. The crushing force vs. deformation responses of the HS-08, HS-18 and HS-19.

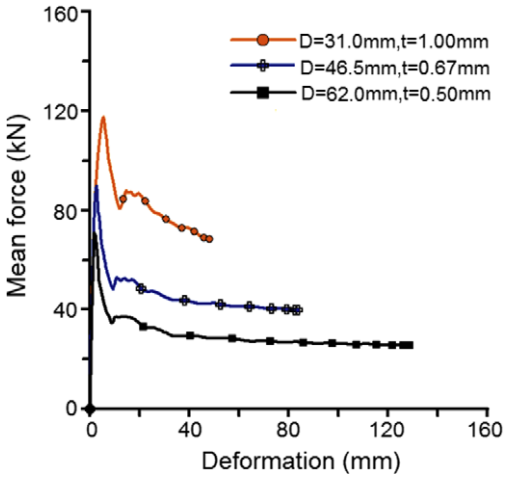

Fig. 17. The mean crushing force vs. deformation responses at different solidity ratio.

$$\phi = \frac{A}{A_1} \tag{7}$$

where A denotes the net section area of the thin-walled tube, and A_1 is the total area. For a constant section area, increasing the diameter of the HS-20 cylindrical thin-walled tube, 31 mm, by factors of 1.5 and 2, yields two cylindrical thin-walled tubes, HS-21and HS-22, respectively, with diameters of 46.5 and 62 mm. The solidity ratio changes to 0.44 times and 0.25 times the original value, respectively. The resulting mean force vs. displacement curve in Fig. 17 indicates the effect of the solidity ratio on the energy absorbing performance of the component, indicating that as the solidity ratio declines, the maximum mean force declines from the original 117.43 to 89.68 kN and eventually to 70.91 kN: it thus decreases by 25–30% as the solidity ratio decreases. The variation of displacement is also large. Accordingly, if the thickness of the structure does not suffice to prevent plastic crushing of the component, the solidity ratio must be considered as an important parameter in determining the size of the designed component for a particular valid area, to enable thin-walled tubes of the same material to absorb more energy and thus be more economical.

5. Conclusions

A non-linear finite element analysis program was adopted to analyze high-strength thin-walled cylindrical tubes. The following conclusions are drawn.

1. Changing the impact mass changes only the impact energy and consequently affects the overall deformation of the component. It does not significantly affect the energy absorbing efficiency of the energy absorbing component.
2. If the thin-walled component is crushed, then a change in the thickness of the thin-walled tube will directly influence the section area that sustains the impact. At the time of impact, the thickness increases and the deformation of the component declines, but can absorb all of the impact energy, indicating that thickness affects energy absorbing efficiency more strongly.
3. Changing the impact speed directly changes the impact energy and causes a discrepancy between mean force and peak loading. At a given impact energy remains, the impact speed and impact mass were changed simultaneously. Analysis outcomes show that impact kinetic energy is more sensitive to speed than is impact mass, which fact also importantly determines energy absorption.
4. When the thin-walled component is buckling, energy absorption increases performance with the solidity ratio. Therefore, considering the solidity ratio into designing the geometry of the structure enables the energy absorbing ability of a particular material to be improved.

References

[1] J.M. Alexander, An approximate analysis of the collapse of thin cylindrical shells under axial loading, The Quarterly Journal of Mechanics and Applied Mathematics 13 (1960) 10–15.
[2] J. Marsolek, H.G. Reimerdes, Energy absorption of metallic cylindrical shells with induced non-axisymmetric folding patterns, International Journal of Impact Engineering 30 (2004) 1209–1212.
[3] A. Singace, H. Elsobky, Further experimental investigation on the eccentricity factor in the progressive crushing of tubes, International Journal of Solid and Structures 33 (1996) 3517–3538.
[4] N. Gupta, Consideration of axisymmetric axial collapse of round tubes, International Journal of Solid and Structures 34 (1997) 2611–2630.
[5] Z.G. Wei, J.L. Yu, R.C. Batra, Dynamic buckling of thin cylindrical shells under axial impact, International Journal of Impact Engineering 32 (2005) 575–592.
[6] K.R.F. Andrews, G.L. England, E. Ghani, Classification of the axial collapse of cylindrical tubes under quasi-static loading, International Journal of Mechanical Sciences 25 (1983) 687–696.
[7] D. Karagiozova, N. Jones, Dynamic buckling of elastic-plastic square tubes under axial impact-II: structural response, International Journal of Impact Engineering 30 (2004) 167–192.
[8] N. Jones, Structural Impact, Cambridge University Press, Cambridge (UK), 1989.
[9] M. Langseth, O.S. Hopperstad, T. Berstad, Crashworthiness of aluminum extrusions: validation of numerical simulation, effect of mass ratio and impact velocity, International Journal of Impact Engineering 22 (1999) 829–854.
[10] M. Yamashita, M. Gotoh, Y. Sawairi, A numerical simulation of axial crushing of tubular strengthening structures with various hat-shaped cross-sections of various materials, Key Engineering Materials 233 (2002) 193–198.
[11] Galib. DAl, A. Limam, Experimental and numerical investigation of static and dynamic axial crushing of circular aluminum tubes, Thin Walled Structures 42 (2004) 1103–1137.
[12] N. Peixinho, A. Pinho, Study of viscoplasticity models for the impact behavior of high-strength steels, Transactions of the ASME 2 (2007) 114–123.
[13] M. Yamashita, M. Gotoh, Y. Sawairi, Axial crush of hollow cylindrical structures with various polygonal cross-sections numerical and experiment, Journal of Materials Processung Technology 140 (2003) 59–64.
[14] A. Rossi, Z. Fawaz, K. Behdinan, Numerical simulation of the axial collapse of thin-walled polygonal section tubes, Thin-Walled Structures 43 (2005) 1646–1661.
[15] R. Rajendran, A. Moorthi, S. Basu, Numerical simulation of drop weight impact behaviour of closed cell aluminium foam, Materials and Design 30 (2009) 2823–2830.
[16] Z. Ahmad, D.P. Thambiratnam, Crushing response of foam-filled conical tubes under quasi-static axial loading, Materials and Design 30 (2009) 2393–2403.
[17] H.L. Fan, D.N. Fang, Enhancement of mechanical properties of hollow-strut foams: analysis, Materials and Design 30 (2009) 1659–1666.
[18] H. Yu, Y. Guo, X. Lai, Rate-dependent behavior and constitutive model of DP600 steel at strain rate from 10–4 to 103 s^{-1}, Materials and Design 30 (2009) 2501–2505.
[19] J.D. Campbell, Dynamic plasticity: macroscopic and microscopic aspects, Materials Science Engineering 12 (1973) 3–21.
[20] J. Duffy, Testing techniques and material behavior at high rates of strain, in: J. Harding (Ed.), Institute of physics Conference Series No. 47 (1979) 1–15.
[21] G.R. Cowper, P.S. Symond, Strain hardening and strain rate effects in the impact loading of cantilever beams, Brown University, Division of applied mathematics report, No. 28, 1957.
[22] P.S. Symond, Survey of methods of analysis for plastic deformation of structures under dynamic loading, Brown University, Division of engineering report, BU/NSRDC/1–67, 1967.
[23] D. Karagiozova, N. Jones, Dynamic elastic-plastic bucking of circular cylindrical shells under axial impact, International Journal of Solids and Structures 37 (2000) 2005–2034.
[24] J. Mark, F.G. Holst, J. Michael Rotter, Axially compressed cylindrical shells with local settlement, Thin-Walled Structures 43 (2005) 811–825.
[25] W. Abramowicz, N. Jone, Dynamic progressive bucking of circular and square tubes, International Journal of Impact Engineering 4 (1986) 243–270.
[26] M. Langseth, O.S. Hopperstad, Static and dynamic axial crushing of square thin-walled aluminium extrusions, International Journal of Impact Engineering 18 (1996) 949–968.